

# A DFT and TD-DFT Study on Emodin and Purpurin and their Functionalized Molecules to Produce Promising Organic Semiconductor Materials

*By Sahar Abdalla etal*

67

# A DFT and TD-DFT Study on Emodin and Purpurin and their Functionalized Molecules to Produce Promising Organic Semiconductor Materials

36

## Abstract

Density functional theory (DFT) computations were done to explore the optical and electronic properties of two conjugated molecules, emodin and purpurin, as potential organic semi-conductors. The molecules were functionalized to explore the impact of functionalization on the electronic and optical properties. The properties calculated include reorganization energy ( $\lambda_h$  and  $\lambda_e$ ), adiabatic ionization potential (IP), adiabatic electron affinity (EA), chemical hardness ( $\eta$ ), HOMO and LUMO energies, and HOMO-LUMO energy gap ( $E_g$ ) via B3LYP/6-3++G (d, p) method. In addition, the maximum absorption ( $\lambda_{max}$ ) and oscillator strength ( $f$ ) at the excited states in vacuum and solvent (Ethanol) were investigated using time-dependent density functional theory (TD-DFT). The introduction of functional groups to emodin was considered to convert the molecule from a p-type into an n-type material, while purpurin is considered as an n-type material, its functionalization with NO<sub>2</sub> and 2F resulted in a slight increase in  $\lambda_e$  values, which is considered detrimental for the process of charge-transport. However, the functionalized molecules have shown an increase in EA and a decrease in LUMO energy level, indicating their potential use as n-type materials. Furthermore, to have an understanding of the intermolecular interactions in emodin and purpurin molecules, Hirshfeld surface analysis and energy framework were studied.

Keywords: Organic semiconductors; Optical properties; Electronic properties; DFT; TD-DFT

**Abbreviation**

HOMO	<sup>11</sup> Highest Occupied Molecular Orbital
LUMO	Lowest Occupied Molecular Orbital
$\lambda$	Reorganization energy
$\lambda_{int}$	Internal reorganization energy
$\lambda_{ext}$	External reorganization energy
IE	Adiabatic Ionization energy
EA	Adiabatic Electron affinity
Eg	Energy gap
DFT	<sup>72</sup> Density functional theory
TD-DFT	Time Dependent - Density functional theory
$\eta$	Chemical Hardness
$\lambda_{max}$	Maximum Absorption
$f$	Oscillator Strength
$\text{\AA}$	Bond lengths
$^{\circ}$	Bond angles
B3LYP	Becke, 3-parameter, Lee-Yang-Parr

## 1 Introduction

The Earth receives a total quantity of radiant energy from the sun of 1370 W/m<sup>2</sup>/s, with 343 W/m<sup>2</sup>/s received per unit area of the Earth's surface [1]. The abundance and non-polluting characteristics of solar energy have made it a widely recognized renewable source of energy. The photovoltaic effect of solar cells can convert this solar energy into electrical energy. Organic solar cells are being increasingly attractive due to their low production cost [2–4], electronic features such as light absorption and emission, charge generation and transportation [5], tuning of molecular properties by modifying the length and type of functional groups [5–8].

The basic operating principle of organic solar cells is the initial absorption of incident photons that leads to the generation of free electrons and holes (excitons) [4, 9]. The Coulomb forces of attraction between the generated excitons are high owing to the low dielectric constant of organic semi-conductors. Therefore, the excitons dissociation requires a heterojunction that is created by two dissimilar organic semi-conductor materials; donor (n-type) and acceptor (p-type). A donor is defined as a material that has a high ionization energy (IP) and an acceptor is a material that has a high electron affinity (EA). Finally, upon the dissociation of excitons, the electron created is transferred to the cathode, and the hole is transferred to the anode to initiate current [9–11].

The most essential features of organic semiconductors are inclusive of abundance and low production cost, optimum energy gap ( $E_g$ ) between HOMO and LUMO, strong light absorption, thermal and photo stability [12–14]. However, there remains the challenge of enhancing the proficiency of solar organic cells in comparison to inorganic solar cells. Several research efforts are being carried out on organic solar cell systems to improve their efficacy, processing and stability [9, 15, 16]. One of the approaches used is to enhance the optical and electronic properties of organic semiconductor molecules by using functional groups to tune their properties [6]. For instance, it was stated that the introduction of electron-deficient atoms or groups increases the molecule electron affinity by reducing the molecular LUMO and thus resulting in better n-type organic semi-conductors. These functional groups include imides, amides, carbonyls, quinones and halogen atoms [9]. To increase the environmental stability and electron affinity of conjugated systems, imides and amides are introduced into the backbone of the molecule as strong electron-withdrawing groups [17]. In a study conducted by Zhenan *et al.*, a p-type material, metallophthalocyanine, was converted into an n-type air-stable material by functionalization with fluorine [18]. Other research showed the pentacene perfluorination converted it into an n-type material [19], while the chloro (Cl) and Nitro (N) functionalization of naphthalene and pentacene molecules provided a better material than perfluoropentacene and octafluoronaphthalene [6, 20]. The addition of the F and CN groups to 1,3,5-tripyrrolebenzene (TPB) have stabilized frontier molecular orbital and improved air stability [21]. In addition, the influence of functionalization on absorption was reported by R. Cardia *et al.* [5] in functionalized triisopropylsilylethynyl (TIPS), resulting in better visible region absorption. This improvement of absorption in the visible region was also shown by different sensitizers functionalized by OH, NH<sub>2</sub>, OCH<sub>3</sub>, CF<sub>3</sub>, F, and CN [22].

Reorganization energy, which is known to influence the rate of charge transfer [23], is a critical element that dictates the efficiency of organic solar cells. The reorganization energy is often considered as the summation of internal and external influences. The internal reorganization energy ( $\lambda_{int}$ ) is attributed to the change in equilibrium geometry of the donor and acceptor sites due to electron transfer, while the external reorganization energy ( $\lambda_{ext}$ ) is attributed to the polarization effects that lead to the change in the surrounding media [8, 23, 24]. The external reorganization energies values are considered to be much smaller than the inner reorganization energies, and thus negligible [21,25,26].

The effect of functionalization on the reorganization energy has been reported by many studies. For example, Hutchison *et al.* [27] investigated the functionalization impact of oligomers of thiophene and furan in terms of reorganization energy. Others have revealed that the cyanation of pentacene gives smaller values of hole (75 meV) and electron reorganization energy (87 meV) than pentacene (94 and 133 meV, respectively) [28]. Oshi and co-workers discussed the increase of hole and electron reorganization energy in 7,7,8,8-Tetracyanoquinodimethane by electron-donating groups CH<sub>3</sub>, OCH<sub>3</sub>, and OH [8]. Thus, it is valuable to recognize the effect of functionalization on molecule's reorganization energy as it provides perception into charge transfer rate in organic semiconductor materials. Charge transport (at low temperatures) in organic semiconductors is described as band-like motion in which the charge is delocalized across the system. The charge transport technique at high temperatures is represented by a hopping mechanism where the charge transporters are localized to a single molecule, and jump from a molecule to a nearby molecule as described by the Marcus equation, which is given as follows: [7, 29–32]

$$K = (4\pi^2/h)t^2(4\pi\lambda K_B T)^{-0.5} \exp[-\lambda/4K_B T]$$

where  $t$ ,  $\lambda$  and  $T$  represent the charge transfer matrix element, reorganization energy and absolute temperature, respectively. While  $h$  and  $K_B$  are the Planck and the Boltzmann constants respectively.

The charge transport rate from the equation is mostly affected by the reorganization energy and electronic coupling (transfer integral). The charge transport rate is determined by the transfer integral, which is influenced by the orientation and distance of the molecules. A lower reorganization energy and larger transfer integral lead to a faster charge transport rate. [31,33,34].

Quantum mechanics and molecular modeling give an understanding of the structure, optical and electronic properties relationships that lead to systematic molecular design [16, 17, 35–37]. In this investigation, the influence of functionalization on electronic and optical properties of two conjugated molecules, emodin (6-methyl-1,3,8-trihydroxyanthraquinone), and purpurin (1,2,4-Trihydroxyanthraquinone) are studied to understand their possible use in organic solar cells, figure 1 and figure 2, respectively. Also, some of the bond lengths (Å) along with the bond angles (°) of emodin and purpurin and their derivatives are presented in Table 4 and Table 5, respectively. Both molecules belong to the anthraquinones, which are considered to be the largest occurring quinones that are naturally abundant. They are used as natural colorants as well as in variety of other applications [38,39].

## 2 Materials and Methods

The structures of emodin and purpurin were optimized via DFT method [40] using Becke, 3-parameter, Lee–Yang–Parr (B3LYP) functional [41-44] and the 6-31++G (d, p) basis set. The B3LYP has been used in the calculation of reorganization energy in several studies [20, 33, 45, 46]. The frequency calculations carried out at the same level of theory, reveal that all studied molecules have reached local minima with no imaginary frequencies. The performed calculations included  $\lambda$  for holes and electrons, adiabatic ionization potential (IP), and adiabatic electron affinity (EA), chemical hardness ( $\eta$ ), HOMO and LUMO energy levels, and energy gap ( $E_g$ ). The reorganization energies for holes ( $\lambda_h$ ) and electrons ( $\lambda_e$ ) are calculated as follows:

$$\lambda_e = (E_0^- - E^-) + (E_-^0 - E_0^0)$$
$$\lambda_h = (E_0^+ - E^+) + (E_+^0 - E_0^0)$$

where the  $E_0^-$  ( $E_0^+$ ) represent the anionic (cationic) energy of the molecule in an optimized neutral structure, the  $E^-$  ( $E^+$ ) is the anionic (cationic) energy of the molecule in an optimized anion (cation) structure, the  $E_-^0$  ( $E_+^0$ ) is the neutral energy of the molecule in optimized anion (cation) structure and the  $E_0^0$  is the neutral energy of the molecule in optimized neutral structure [34, 47, 48].

The IP and EA energies were calculated as per the following equation:

$$IP = E(M^+) - E(M^0)$$
$$EA = E(M^0) - E(M^-)$$

The  $E(M^0)$ ,  $E(M^-)$  and  $E(M^+)$  represents the total energies of the neutral, anionic, and cationic state of the molecule [6]. The chemical hardness of the molecule,  $\eta$ , was calculated using  $\eta = \frac{IP-EA}{2}$  [12, 49].

The excited states of the molecules were determined using time-dependent density functional theory (TD-DFT) [50] utilizing the B3LYP functional with 6-31++ (d, p) basis set from ground state optimized geometry in vacuum and solvent (Ethanol). This gives the absorption spectra and oscillator strength. All calculations were done using Gaussian 09 program [51].

Furthermore, the intermolecular interaction of emodin and purpurin were investigated to determine the role of these interactions to the crystal lattice through Hirshfeld surface analysis [52]. To aid the interpretation of the interactions,  $d_{\text{map}}$ , shape index and 2D fingerprint plots [52] were demonstrated. The 3D energy framework was represented by computing the interaction energies, electrostatic energy, polarization energy, dispersion energy, exchange-repulsion energy, and total intermolecular energy [53] at B3LYP/6-31G (d,p), and a 3.8 Å cluster was generated around the molecule. The calculations were done using the CrystalExplorer17 program [54]. Emodin and hydrated purpurin was used in the representation of the 3D energy framework.

### 3 Results and Discussion

#### 3.1 Reorganization Energy

The  $\lambda_h$  and  $\lambda_e$  values of emodin and its functionalized molecules are listed in Table 1. For emodin, it can be observed that the  $\lambda_h$  value is smaller than the value of  $\lambda_e$ , 0.22 eV and 0.41 eV, respectively. The  $\lambda_h$  values increased upon the introduction of functional groups, with the lowest value being 0.38 eV for molecules 4 and 5, and the highest value being 0.40 eV for molecules 2 and 3. The  $\lambda_e$  showed only a slight change in values with an increase of 0.03 eV on F-functionalized molecule 4 and a decrease for molecules 3 (0.03 eV) and 5 (0.01 eV). The changes in  $\lambda_h$  and  $\lambda_e$  are due to the changes in structure during oxidation and reduction that are attributed to the C-X (functional groups), bonds contribution. As mentioned in section 1, the charge transfers rate increases with the decrease of reorganization energy. As such, emodin without functionalization is predicted to have the highest charge transfer rate and serves as a good candidate as a hole transport material and electron transport material upon the introduction of functional groups.

Purpurin  $\lambda_h$  and  $\lambda_e$  values are also listed in Table 1. Unlike emodin, the value of  $\lambda_e$  is smaller than  $\lambda_h$  value, 0.39 eV and 0.59 eV, respectively. Accordingly, purpurin without functionalization may act as a good electron transport material. The addition of functional groups has led into a minor decrease of  $\lambda_h$  in molecules 2, 3, 5 and 6 with  $\lambda_h$  values of 0.56, 0.56, 0.58, and 0.58 eV, respectively. The only increase was in Cl-functionalized molecule 4, with  $\lambda_h$  to be 0.60 eV. The changes in  $\lambda_e$  values are also minor, with the largest increase for molecules 2 and 6 by 0.03 eV and the smallest decrease for molecule 3 by 0.02 eV. While no change occurred in the Cl-functionalized molecules, 4 and 5. Based on the given data, purpurin is inclined to have a high charge transport rate as an electron transport material and its functionalized molecules may also have a similar charge transfer rate as electron transport materials.

In general, for halogenated molecules, the values for F show higher reorganization energy than Cl, in emodin and purpurin as a result of the higher electronegativity of Fluorine. This is in agreement with results of halogenated naphthalene [6] and tetracene [55]. It is suggested that the intra-ring functionalization of molecules may yield better results in minimizing the reorganization energy as it avoids the introduction of additional degrees of freedom for geometric relaxation [23]. Overall, the values of  $\lambda_h$  and  $\lambda_e$  are similar to those of proposed organic semiconductors [6–8,23]. The values of chemical hardness for the two molecules are also presented in Table 1. The chemical hardness ( $\eta$ ) is defined as the resistance of the chemical potential to change in the number of electrons [47], the functionalized molecules show similar values of  $\eta$  to that of emodin and purpurin, indicating their stability.



### 3.2 Adiabatic Ionization Potential and Adiabatic Electron Affinity

The values IP and EA for emodin, purpurin, and their functionalized molecules are illustrated in Table 1. One of the concerns in n-type organic semiconductor systems is the lack of stability of their radical anions in the air, [56] and functionalization of molecules may be used to tune IP and EA values for a more stabilized molecule. The IP value of emodin is calculated to be 8.74 eV and the EA is 1.85 eV, and because of the similarity in structure, the IP and EA of purpurin have shown similar values to that of emodin with values of 8.43 eV and 1.85 eV, respectively.

The functionalization of emodin and purpurin results in a decrease of IP and an increase in EA values. The values of emodin IP are in the sequence of molecules 1 > 3 > 5 > 4 > 2 and for EA values 3 > 5 > 4 > 2 > 1 and for purpurin the IP values are in the sequence of 1 > 2 > 3 > 6 > 5 > 4 and for EA 2 > 3 > 5 > 6 > 4 > 1. The NO<sub>2</sub>-functionalized purpurin has the highest IP and EA values due to the negative resonance effect and electron affinity of the NO<sub>2</sub> group. Electrons are withdrawn from the rings, leading to electron deficit at all positions of the fused rings. It is followed by the CN-functionalized molecule, which is attributed to the interactions of the nitrogen lone pair of electrons (negative resonance effect) with the  $\pi$ -electron clouds of the fused rings, as well as the inductive effect of the electronegative nitrogen atom. These results are in agreement with the NO<sub>2</sub> and CN functionalization of tetracene [7].

Similarly, the CN-functionalized molecule in emodin has the highest EA value, 2.33 eV. The 2Cl-functionalized purpurin molecule has a higher EA value than the 2F-functionalized molecule, that is accounted for by the higher ability of Cl to withdraw electrons, taking into consideration resonance and inductive effects. This is in agreement with halogenated pentacene [20] and naphthalene [6]. In addition, the Cl-functionalized emodin molecule also has a higher EA than the F-functionalized molecule.

### 3.3 HOMO and LUMO Energy, and Optical properties

The values of  $E_g$ , HOMO and LUMO of emodin, purpurin and their functionalized molecules are shown in Table 2. The molecules  $E_g$  falls within the range of organic semiconductors, 1.4 - 4.2 eV [34]. The functionalization of emodin and purpurin contributed to lowering the energy gap that predicts kinetic stability and an increase in conductivity.

The energy gap of emodin and its functionalized molecules ranged between 3.40 - 3.52 eV, the smallest  $E_g$  value was for CN-functionalized molecule 3, 3.40 eV, followed by Cl-functionalized molecule 5, 3.45 eV, and accordingly is predicted to have better conductivity. In addition, the LUMO energy levels and  $\lambda_c$  of CN and Cl-functionalized molecules also have the lowest values, which results in improved emodin functionality as an n-type material.

The overall LUMO values decreased except for the functionalized C<sub>2</sub>H<sub>2</sub> molecule. The LUMO values ordered as molecule 1 = 2 > 4 > 5 > 3. The CN-functionalized molecule showed the lowest value, leading to the smallest energy gap value. The HOMO levels also decreased in value with the order of molecule 1 = 2 > 4 > 5 > 3. The HOMO and LUMO values of purpurin and its functionalized molecules are in the sequence of molecule 1 > 4 > 5 > 6 > 3 > 2 and 1 > 4 > 6 > 5 > 3 > 2, respectively. The  $E_g$  values range from 2.84 - 3.12 eV, emodin showed the highest  $E_g$  value of 3.12 eV with NO<sub>2</sub>- functionalization. The value decreased into 2.84 eV to become the smallest  $E_g$  among the molecules, followed by the CN-functionalized molecule 3.



The decrease in  $E_g$  values of emodin and purpurin upon the addition of functional groups is in consistent with the results obtained for F, CN Cl, and  $\text{NO}_2$  functionalized tetracene and anthracene by [7]. Overall, the LUMO values of the molecules are in the range of typical n-type materials between -3.0 and -4.0 eV, lowering of LUMO also results in an increase in stability [23] and a higher ability to accept electrons [49]. Hence, the studied molecules are proposed to be good n-type materials. The study of these frontier molecular orbitals (FMO), in qualitative manner, are insightful in predicting the electron transition [47]. Therefore, the HOMO and LUMO qualitative molecular representations of emodin, purpurin and their functionalized molecules in  $S_0$  are represented in figures 3 and 4. For emodin and its functionalized molecules, the HOMO and LUMO are delocalized on one of the benzene rings and slightly on the functionalized benzene ring. This indicates a strong overlap between the HOMO and LUMO that leads to strong optical absorption due to electron excitation  $S_0$ - $S_1$ . For purpurin, the HOMO and LUMO are delocalized on one of the benzene ring, the transition is mainly within the non-functionalized benzene ring. The electrostatic potential (ESP) is useful in predicting the reactive sites of the molecule. The ESP of the molecules increases in the order of red > orange > yellow > green > blue. The reactive sites of the emodin, purpurin and their functionalized molecules are also shown in figure 5. In general, the addition of the functionalization resulted in an increase in reactivity in the site except for molecule 2 in emodin.

The oscillator strengths of emodin, purpurin and their functionalized molecules are presented in Table 3. Oscillator strength expresses the probability of absorption of electromagnetic radiation, the higher the oscillator strength is for a molecule the higher the expected absorption. In this study, the strongest absorption for emodin corresponds to excited state  $S_1$  with a value of 413.28 nm ( $f=0.1139$ ) in a vacuum. For molecule 2, the strongest absorption was at excited state  $S_1$  with a value of 429.11 nm ( $f=0.1427$ ) in the solvent. The strongest absorption in molecule 3 corresponds to 439.71 nm ( $f=0.1168$ ) in the solvent at excited state  $S_1$ . The excited state  $S_1$  shows the strongest absorption for molecule 4 with a value of 425.47 nm ( $f=0.1283$ ) in the solvent. Finally, molecule 5 also shows the strongest absorption at excited state  $S_1$  with a value of 434.66 nm ( $f=0.146$ ) in the solvent.

For purpurin, the excited state ( $S_1$ ) corresponds to the maximum absorption with values of 461.81 nm ( $f=0.194$ ) in the solvent. For  $\text{NO}_2$ - functionalized molecules, the strongest absorption value is 541.1 nm ( $f=0.0944$ ) in the solvent at excited state  $S_1$ . For molecules 3, 1022.69 nm ( $f=0.297$ ) in the solvent at excited state  $S_1$ . For the 1Cl-functionalized molecule at excited state  $S_1$  with a value of 466.58 nm ( $f=0.2031$ ) in the solvent. As for the 2Cl-functionalized molecule, which also corresponds to excited state  $S_1$  with a value of 473.32 nm ( $f=0.2028$ ) in the solvent. For molecule 6, the strongest absorption takes place in a vacuum with a value of 456.44 nm ( $f=0.1241$ ). It can be noticed from the given values in Table 3, that the solvent resulted in a redshift of the maximum absorption. Moreover, the decrease in the  $E_g$  values also resulted in a red shift in the maximum absorption, as listed in Table 2.

### 3.4 Hirshfeld Surface Analysis

The Hirshfeld surface analysis aids in the quantification and visualization of intermolecular interactions by utilizing different colors and intensities in graphical representation. Hirshfeld surface analysis has been used to investigate various intermolecular interactions in the crystal structure of organic molecules and complexes [57, 58]. The  $d_{\text{norm}}$  (normalized

contact distance) maps of emodin and purpurin are depicted in figure 6. The contacts with shorter distances (close contacts) than the Van der Waals radii are represented by red surfaces, while the blue surfaces represent contacts with longer distances (distance contact). The white surfaces denote distance equivalent to the sum of Van der Waals radii. The red regions in emodin and purpurin appears to originate from the -OH groups in the molecules. The red regions of the molecules may act as donors in intermolecular reactions. Thereby, it is expected that their functionalized molecules with electronegative groups would adhere more sites that act as donors. The shape-index of emodin and purpurin on the Hirshfeld surface is presented in figure 7. The red and blue regions represent the donor and acceptor groups of the molecule, the adjacent red and blue triangles denote  $\pi$ - $\pi$  stacking interaction among the structures.

The 2D fingerprint plots and fragment patches of emodin and purpurin are illustrated in figures 8 and 9, respectively. The  $d_e$  and  $d_i$  on the plots represent the distances to the nearest atom center, external and internal to the surface. Points on the plot without contribution are gray colored and points with small contribution is blue colored through green to red for the points with the largest contribution. The most significant interaction in emodin is O--H/H--O that contributes 31.8 % to the overall surface. The second largest interaction is H--H with contribution of 30.1 % as pair wings, followed by C--H/H--C (15.9 %), C--C (10.9 %) and O--C/C--O (9.1 %). In purpurin, the O--H/H--O interactions dominated with a contribution of 41%, while the H--H and C--C interactions were 26.6% and 22.3%, respectively. Both molecules have other small contributions; emodin O--O (2.2%) and purpurin C--H/H--C (5.5%), O--O (2.8%) and C--O/O--C (1.9%).

### 3.5 Energy Frameworks

The calculated interaction energies energy  $E_{tot}$  ( $\text{kJ mol}^{-1}$ ) namely, electrostatic ( $E_{elec}$ ), polarization ( $E_{pol}$ ), dispersion ( $E_{dis}$ ), exchange-repulsion ( $E_{rep}$ ) are used to generate 3D representation of the major interactions in the form of energy frameworks. figure 10 The interaction energies relative strength in individual directions are represented by exhibited cylinder-shaped energy frameworks, the size of the interactions that are less than  $5 \text{ kJ mol}^{-1}$  have been excluded. It can be seen that the intermolecular interactions are dominated by dispersion forces in emodin and purpurin, figure 9 and figure 10, respectively.

### 4.4 Conclusion

In the present paper, the electronic and optical properties of emodin and purpurin were investigated utilizing DFT and TD-DFT methods, to learn about their possible use as organic semiconductors. The molecules were also functionalized by electronegative groups to appreciate the influence of functionalization on the optical and electronic properties of the molecules. There was an overall increase in reorganization energy due to the geometrical changes of the molecule upon oxidation and reduction processes. However, the decrease in  $E_g$  and LUMO energy levels of the molecules predicts the increase in stability and conductivity. Furthermore, an increase in EA values was also noted to reinforce the molecule's ability to accept electrons. Hence, the functionalization of emodin and purpurin strengthened the n-type properties of the molecules. The energy gaps of the molecules are within the range of semi-conductors (1.4 - 4.2 eV)

and the absorption ranges of the molecules are within the visible range. Based on the given data, we have concluded that emodin and purpurin along with their functionalized molecules are good candidates for organic semi-conductors. Also, the intermolecular interactions and 3D energy framework of emodin and purpurin molecules were studied through Hirshfeld surface analysis. It has been shown that the main interaction in the crystal structure of emodin and purpurin is O--H/H--O and dispersion energy was dominant in the 3D energy framework.

## **5 Acknowledgment**

We would like to thank all our colleagues from Sudan University, Khartoum University and Jubail Industrial College for all their support. This study received no specific grant from public, private, or non-profit funding agencies.

## Figure and Table legends

Figure 1: Structure and numbered atoms of emodin, 6-methyl-1,3,8-trihydroxyanthraquinone

Molecule 1: R15= R16= R17= R18= R19= R26= CH<sub>3</sub>

Molecule 2: R26= C<sub>2</sub>H<sub>5</sub>

Molecule 3: R15= CN

Molecule 4: R15= F

Molecule 5: R26= Cl

Figure 2: Structure and numbered atoms of purpurin, 1,2,4-Trihydroxyanthraquinone

Molecule 1: R17= R18= R19= R20= R21= H

Molecule 2: R18= NO<sub>2</sub>

Molecule 3: R18= CN

Molecule 4: R18= Cl

Molecule 5: R17= R18= Cl

Molecule 6: R17= R18= F

Figure 3: HOMO and LUMO of emodin molecule 1 – 5

Figure 4: HOMO and LUMO of purpurin molecule 1 – 6

Figure 5: ESP of emodin and purpurin

Figure 6: Hirshfeld surface of emodin and purpurin plotted over  $d_{norm}$  in the range of -0.4160 to 1.2016 and -1.7662 to 0.8459 a.u, respectively

Figure 7: Shape-index of emodin and purpurin on Hirshfeld surface

Figure 8: Emodin two-dimensional fingerprint plots and fragment patches (surface patches adjacent to neighboring surfaces are colored separately) for intermolecular interactions

Figure 9: Purpurin two-dimensional fingerprint plots and fragment patches (surface patches adjacent to neighboring surfaces are colored separately) for intermolecular interactions

Figure 10: Emodin and purpurin energy frameworks, coulomb energy (red), dispersion energy (green) and total energy (blue)

Table 1:  $\lambda_h$  and  $\lambda_e$ , IP, EA and  $\eta$  (in eV) of emodin and purpurin and their derivatives calculated at B3LYP/6-31++G (d,p) level of theory

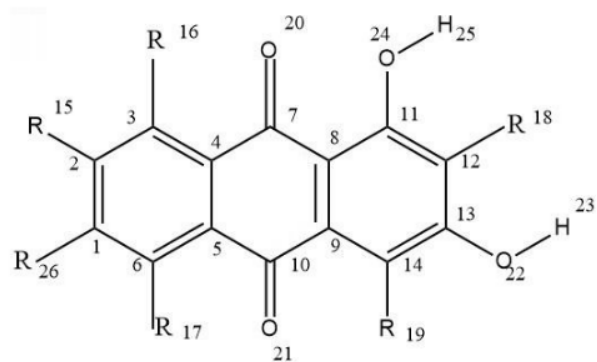
Table 2: HOMO-LUMO Gap of Indigo, Alizarin and derivatives

Table 3: Maximum absorption and oscillator strength of emodin and purpurin along with their derivatives in presence and absence of ethanol solvent

Table 4: Some of the bond lengths (Å) and bond angle (°) of emodin and its functionalized derivatives calculated at the B3LYP/6-31++G(d,p), for the structures and atom numbering, see Fig 1.

Table 5: Some of the bond lengths (Å) and bond angle (°) of purpurin and their functionalized derivatives calculated at the B3LYP/6-31++G(d,p), for the structures and atom numbering, see Fig 2.

Figures



19

Figure 1: Structure and numbered atoms of emodin, 6-methyl-1,3,8-trihydroxyanthraquinone

Molecule 1: R15= R16= R17= R18= R19= R26= CH<sub>3</sub>

Molecule 2: R26= C<sub>2</sub>H<sub>5</sub>

Molecule 3: R15= CN

Molecule 4: R15= F

Molecule 5: R26= Cl

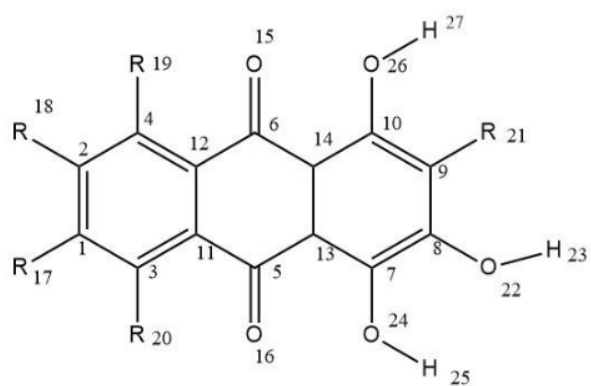


Figure 2: Structure and numbered atoms of purpurin, 1,2,4-Trihydroxyanthraquinone

Molecule 1: R17= R18= R19= R20= R21= H

Molecule 2: R18= NO<sub>2</sub>

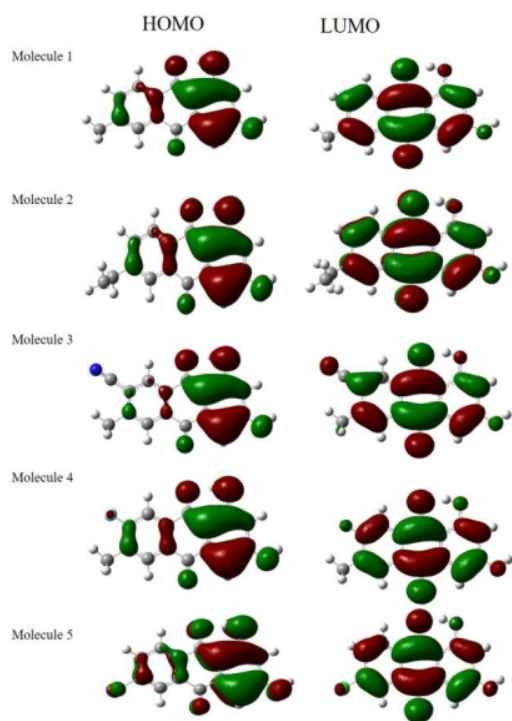
Molecule 3: R18= CN

Molecule 4: R18= Cl

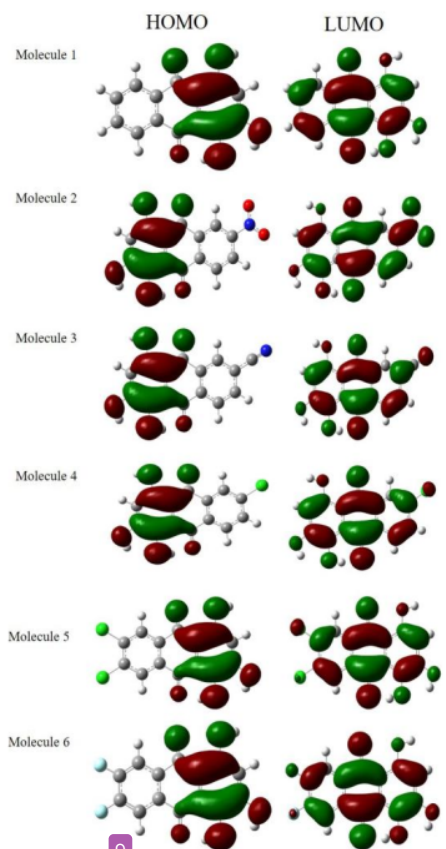
Molecule 5: R17= R18= Cl

Molecule 6: R17= R18= F



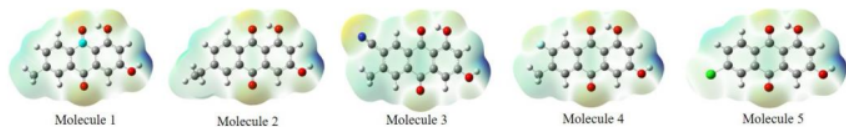


9  
 Figure 3: HOMO and LUMO of emodin molecule 1 – 5



9  
Figure 4: HOMO and LUMO of purpurin molecule 1 – 6

Emodin



Purpurin

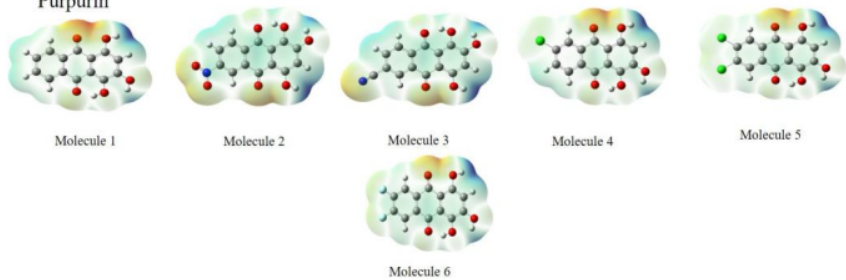
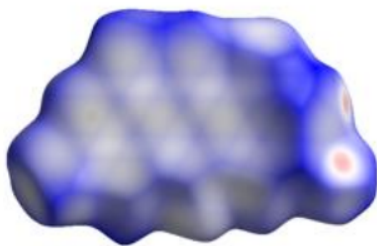


Figure 5: ESP of emodin and purpurin

Emodin



Purpurin

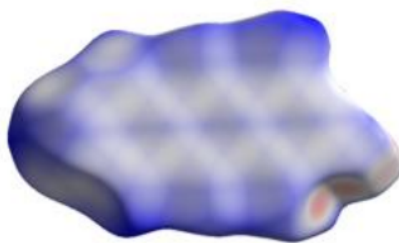
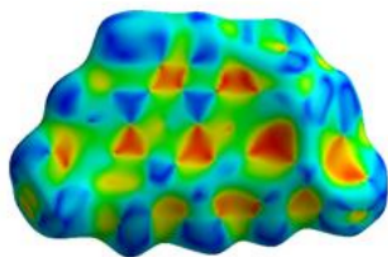


Figure 6: Hirshfeld surface of emodin and purpurin plotted over  $d_{norm}$  in the range of -0.4160 to 1.2016 and -1.7662 to 0.8459 a.u., respectively

Emodin



Purpurin

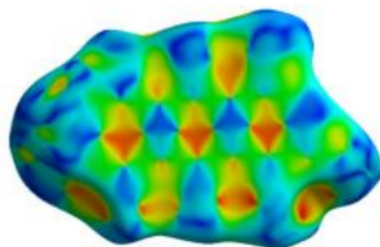


Figure 7: Shape-index of emodin and purpurin on Hirshfeld surface

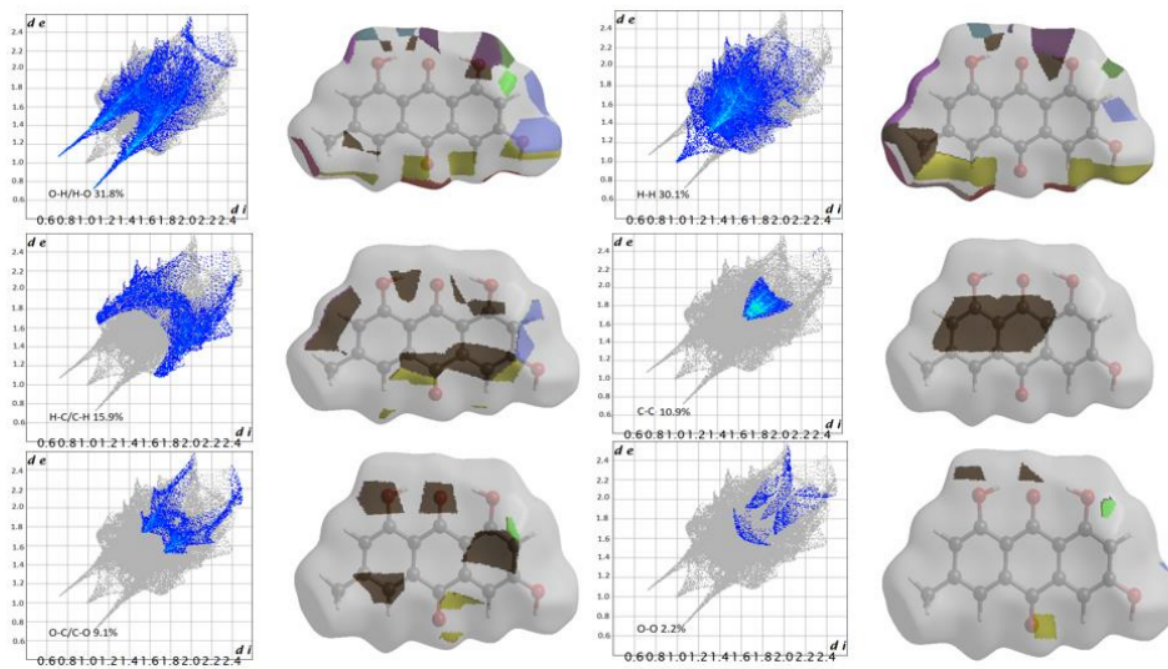


Figure 8: Emodin two-dimensional fingerprint plots and fragment patches (surface patches adjacent to neighboring surfaces are colored separately) for intermolecular interactions



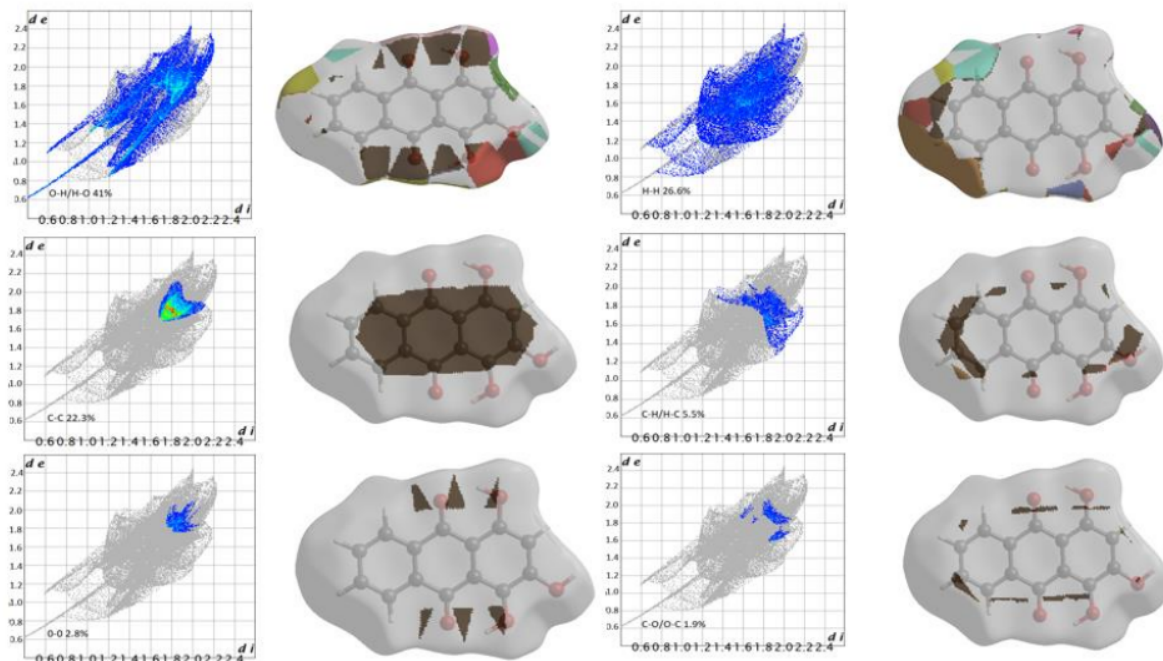


Figure 9: Purpurin two-dimensional fingerprint plots and fragment patches (surface patches adjacent to neighboring surfaces are colored separately) for intermolecular interactions

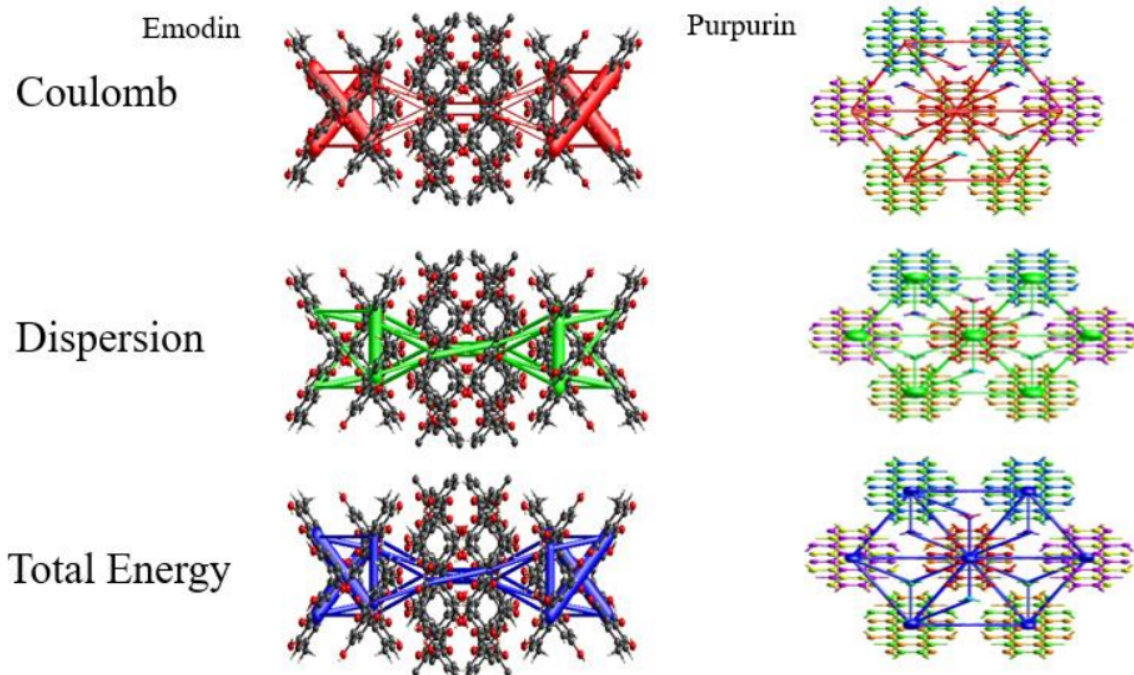


Figure 10: Emodin and purpurin energy frameworks, coulomb energy (red), dispersion energy (green) and total energy (blue)

Molecule	$\lambda_h$	$\lambda_e$	IP	EA	$n$
Emodin					
1 – None	0.22	0.41	8.74	1.85	3.44
2 – (1) Ethylene	0.40	0.41	8.13	1.87	3.13
3 – (1) CN	0.40	0.38	8.42	2.33	3.05
4 – (1) F	0.38	0.43	8.24	1.98	3.13
5 – (1) Cl	0.38	0.40	8.30	2.13	3.09
Purpurin					
1 – None	0.59	0.39	8.43	1.85	3.29
2 – (1) NO <sub>2</sub>	0.56	0.42	8.06	2.59	2.74
3 – (1) CN	0.56	0.37	8.01	2.37	2.82
4 – (1) Cl	0.60	0.39	7.81	2.04	2.88
5 – (2) Cl	0.58	0.39	7.88	2.19	2.85
6 – (2) F	0.58	0.42	7.93	2.12	2.91

Table 1:  $\lambda_h$  and  $\lambda_e$ , IP, EA and  $\eta$ (in eV) of emodin and purpurin and their derivatives calculated at B3LYP/6-31++G(d,p) level of theory

Molecule	<sup>82</sup> E <sub>g</sub> (eV)	$\lambda_{abs}$	HOMO(eV)	LUMO(eV)	<i>f</i>
<b>Emodin</b>					
1 – None	3.52	413.28	-6.69	-3.18	0.1139
2 – (1) Ethylene	3.51	414.72	-6.69	-3.18	0.1173
3 – (1)CN	3.40	427.31	-7.01	-3.62	0.091
4 – (1)F	3.51	411.77	-6.81	-3.30	0.1063
5 – (1)Cl	3.45	421.43	-6.89	-3.44	0.1183
<b>Purpurin</b>					
1 – None	3.12	452.09	-6.31	-3.19	0.1274
2 – (1)NO <sub>2</sub>	2.84	509.51	-6.68	-3.84	0.0797
3 – (1)CN	2.97	480.52	-6.63	-3.66	0.1138
4 – (1)Cl	3.09	455.57	-6.44	-3.35	0.1349
5 – (2)Cl	3.06	461.24	-6.53	-3.47	0.135
6 – (2)F	3.09	456.44	-6.54	-3.45	0.1241

Table 2: HOMO-LUMO Gap of emodin, purpurin and derivatives

Molecule	Excited State 1				Excited State 2				Excited State 3			
	$\lambda_{max}(nm)$	$f$	$\lambda_{max}(nm)$	$f$	$\lambda_{max}(nm)$	$f$	$\lambda_{max}(nm)$	$f$	$\lambda_{max}(nm)$	$f$	$\lambda_{max}(nm)$	$f$
<b>Emodin</b>	Without Solvent		With Solvent		Without Solvent		With Solvent		Without Solvent		With Solvent	
1 – None	413.28	0.1139	419.83	0	388.39	0	407.63	0.175	381.58	0.1036	380.18	0
2 – (1) Ethylene	414.72	0.1173	429.11	0.1427	413.11	0.0003	403.01	0	365.56	0.012	378.55	0.0356
3 – (1) CN	427.31	0.091	439.71	0.1168	417.29	0	408	0	362	0	386.1	0.039
4 – (1) F	411.77	0.1063	425.47	0.1283	409.61	0	399.56	0	356.28	0	380.94	0.0464
5 – (1) Cl	421.43	0.1183	434.66	0.146	412.82	0	402.54	0	360.14	0	383.27	0.026
<b>Purpurin</b>	Without Solvent		With Solvent		Without Solvent		With Solvent		Without Solvent		With Solvent	
1 – None	452.09	0.1274	461.81	0.194	449.76	0	425.89	0	350.37	0	370.06	0.0317
2 – (1) NO <sub>2</sub>	509.51	0.0797	541.1	0.0944	467.25	0	442.21	0	374.59	0.0096	401.81	0.0597
3 – (1) CN	480.52	0.1138	1022.69	0.0297	457.45	0	1011.86	0.001	357.24	0	693.33	0
4 – (1) Cl	455.57	0.1349	466.58	0.2031	446.72	0	423.55	0	366.79	0.0651	379.2	0.0608
5 – (2) Cl	461.24	0.135	473.32	0.2028	447.96	0	424.82	0	373.14	0.0318	382.31	0.0322
6 – (2) F	456.44	0.1241	708.01	0	444.04	0	478.79	0	365.57	0.0265	465.55	0

Table 3: Maximum absorption and oscillator strength of emodin and purpurin along with their derivatives in presence and absence of ethanol solvent

Emodin	Molecule 1	Molecule 2	Molecule 3	Molecule 4	Molecule 5
<b>Bond length (Å)</b>					
C <sub>1</sub> -C <sub>2</sub>	1.404	1.406	1.416	1.400	1.399
C <sub>2</sub> -C <sub>3</sub>	1.393	1.392	1.403	1.386	1.391
C <sub>3</sub> -C <sub>4</sub>	1.399	1.400	1.393	1.396	1.400
C <sub>4</sub> -C <sub>5</sub>	1.410	1.409	1.409	1.409	1.408
C <sub>5</sub> -C <sub>6</sub>	1.397	1.398	1.396	1.398	1.398
C <sub>6</sub> -C <sub>1</sub>	1.401	1.399	1.399	1.399	1.392
C <sub>4</sub> -C <sub>7</sub>	1.483	1.483	1.487	1.485	1.485
C <sub>7</sub> -C <sub>8</sub>	1.457	1.457	1.455	1.455	1.455
C <sub>8</sub> -C <sub>9</sub>	1.420	1.419	1.421	1.420	1.420
C <sub>9</sub> -C <sub>10</sub>	1.497	1.497	1.495	1.498	1.496
C <sub>10</sub> -C <sub>11</sub>	1.421	1.421	1.422	1.421	1.421
C <sub>11</sub> -C <sub>12</sub>	1.402	1.402	1.402	1.402	1.402
C <sub>12</sub> -C <sub>13</sub>	1.392	1.392	1.392	1.392	1.392
C <sub>13</sub> -C <sub>14</sub>	1.407	1.407	1.408	1.407	1.407
C <sub>9</sub> -C <sub>14</sub>	1.385	1.385	1.384	1.384	1.384
C <sub>7</sub> -O <sub>20</sub>	1.250	1.251	1.249	1.249	1.250
C <sub>10</sub> -O <sub>21</sub>	1.226	1.226	1.225	1.227	1.225
<b>Bond Angle (°)</b>					
C <sub>1</sub> C <sub>2</sub> C <sub>3</sub>	121.2	121.2	121.1	123.7	119.2
C <sub>2</sub> C <sub>3</sub> C <sub>4</sub>	120.2	120.2	120.2	118.7	120.5
C <sub>3</sub> C <sub>4</sub> C <sub>5</sub>	119.2	119.2	119.3	119.6	119.5
C <sub>4</sub> C <sub>5</sub> C <sub>6</sub>	119.8	119.8	119.9	119.6	120.1
C <sub>5</sub> C <sub>6</sub> C <sub>1</sub>	121.2	121.2	121.8	122.0	119.2
C <sub>6</sub> C <sub>1</sub> C <sub>2</sub>	118.1	118.1	117.5	116.2	121.3
C <sub>5</sub> C <sub>4</sub> C <sub>7</sub>	121.0	120.9	121.1	121.0	120.9
C <sub>4</sub> C <sub>7</sub> C <sub>8</sub>	118.4	118.5	118.3	118.3	118.4
C <sub>7</sub> C <sub>8</sub> C <sub>9</sub>	121.6	121.6	121.8	121.7	121.7
C <sub>8</sub> C <sub>9</sub> C <sub>10</sub>	120.3	120.3	120.4	120.4	120.3
C <sub>9</sub> C <sub>10</sub> C <sub>5</sub>	117.4	117.5	117.4	117.4	117.4
C <sub>10</sub> C <sub>5</sub> C <sub>4</sub>	120.9	120.9	120.9	121.0	121.0
C <sub>9</sub> C <sub>8</sub> C <sub>11</sub>	118.4	118.4	118.4	118.4	118.4
C <sub>8</sub> C <sub>11</sub> C <sub>12</sub>	120.1	120.1	120.1	120.1	120.1
C <sub>11</sub> C <sub>12</sub> C <sub>13</sub>	119.8	119.8	119.8	119.7	119.8
C <sub>12</sub> C <sub>13</sub> C <sub>14</sub>	121.0	121.0	121.0	121.0	121.0
C <sub>13</sub> C <sub>14</sub> C <sub>9</sub>	119.2	119.2	119.2	119.2	119.2
C <sub>14</sub> C <sub>9</sub> C <sub>8</sub>	121.2	121.1	121.2	121.1	121.2

Table 4: Some of the bond lengths (Å) and bond angle (°) of emodin and its functionalized derivatives calculated at the B3LYP/6-31++G(d,p), for the structures and atom numbering, see Fig 1.



7 purpurin	Molecule 1	Molecule 2	Molecule 3	Molecule 4	Molecule 5	Molecule 6
<b>Bond length (Å)</b>						
$C_1 - C_2$	1.401	1.398	1.410	1.401	1.409	1.401
$C_2 - C_4$	1.393	1.388	1.400	1.391	1.393	1.383
$C_4 - C_{12}$	1.400	1.398	1.397	1.398	1.396	1.400
$C_{12} - C_{11}$	1.407	1.405	1.405	1.406	1.405	1.406
$C_{11} - C_3$	1.403	1.403	1.403	1.403	1.399	1.404
$C_{12} - C_6$	1.503	1.506	1.506	1.505	1.503	1.503
$C_6 - C_{14}$	1.479	1.476	1.476	1.477	1.477	1.477
$C_{14} - C_{13}$	1.433	1.435	1.434	1.434	1.434	1.434
$C_{13} - C_5$	1.467	1.465	1.466	1.469	1.468	1.468
$C_5 - C_{11}$	1.474	1.480	1.478	1.472	1.475	1.474
$C_{14} - C_{10}$	1.408	1.408	1.408	1.408	1.408	1.408
$C_{10} - C_9$	1.409	1.410	1.410	1.409	1.410	1.410
$C_9 - C_8$	1.381	1.381	1.381	1.381	1.381	1.381
$C_8 - C_7$	1.416	1.417	1.417	1.416	1.417	1.417
$C_7 - C_{13}$	1.400	1.401	1.401	1.400	1.400	1.400
$C_6 - O_{15}$	1.228	1.227	1.227	1.227	1.227	1.228
$C_5 - O_{16}$	1.251	1.249	1.249	1.251	1.249	1.250
<b>Bond Angle (°)</b>						
$C_1C_2C_4$	120.3	122.6	120.3	121.5	120.0	120.9
$C_2C_4C_{12}$	120.2	118.7	119.9	119.3	120.5	119.3
$C_4C_{12}C_{11}$	119.3	119.5	119.5	119.8	119.3	119.6
$C_{12}C_{11}C_3$	120.2	120.5	120.3	119.9	120.2	120.5
$C_{11}C_3C_1$	119.9	120.1	120.1	120.3	120.1	118.9
$C_3C_1C_2$	119.9	118.4	119.6	119.0	119.6	120.5
$C_{12}C_6C_{14}$	117.4	117.2	117.2	117.2	117.1	117.2
$C_{11}C_{12}C_6$	122.0	122.2	122.1	122.1	122.2	122.2
$C_6C_{14}C_{13}$	119.9	120.0	120.0	119.9	120.0	119.9
$C_{14}C_{13}C_5$	121.7	121.8	121.8	121.7	121.8	121.8
$C_{13}C_5C_{11}$	118.7	118.7	118.7	118.7	118.5	118.6
$C_5C_{11}C_{12}$	120.0	119.9	119.9	120.1	120.1	120.1
$C_{13}C_{14}C_{10}$	117.9	117.9	117.9	117.9	117.9	117.9
$C_{14}C_{10}C_9$	120.6	120.6	120.6	120.6	120.6	120.6
$C_{10}C_9C_8$	120.9	121.0	121.0	120.9	120.9	120.9
$C_9C_8C_7$	119.8	119.7	119.7	119.8	119.8	119.8
$C_8C_7C_{13}$	119.8	119.7	119.8	119.8	119.7	119.7
$C_7C_{13}C_{14}$	120.8	120.8	120.7	120.7	120.7	120.7

Table 5: Some of the bond lengths (Å) and bond angle (°) of purpurin and their functionalized derivatives calculated at the B3LYP/6-31++G(d,p), for the structures and atom numbering, see Fig 2.

## References

- [1] B. Zaidi, Introductory chapter: Introduction to photovoltaic effect, Solar Panels and Photovoltaic Materials; InTech Open: London, UK (2018) 1–8.
- [2] A. M. Bagher, M. M. A. Vahid, M. Mohsen, Types of solar cells and application, American Journal of optics and Photonics 3 (5) (2015) 94–113.
- [3] R. Jin, K. Wang, Rational design of diketopyrrolopyrrole-based small molecules as donating materials for organic solar cells, International journal of molecular sciences 16 (9) (2015) 20326–20343.
- [4] O. Ourahmoun, M. Belkaïd, Dependence of the characteristics of organic solar cells on cathode polymer interface, Revue des énergies renouvelables 13 (4) (2010) 583–590.
- [5] R. Cardia, G. Mallocci, A. Mattoni, G. Cappellini, Effects of tips-functionalization and perhalogenation on the electronic, optical, and transport properties of angular and compact dibenzochrysene, The Journal of Physical Chemistry A 118 (28) (2014) 5170–5177.
- [6] R. Oshi, S. Abdalla, M. Springborg, Study of the influence of functionalization on the reorganization energy of naphthalene using dft, Computational and Theoretical Chemistry 1099 (2017) 209–215.
- [7] R. Oshi, S. Abdalla, M. Springborg, Theoretical study on functionalized anthracene and tetraceneas starting species to produce promising semiconductor materials, Computational and Theoretical Chemistry 1128 (2018) 60–69.
- [8] R. Oshi, S. Abdalla, M. Springborg, The impact of functionalization of organic semiconductors by electron donating groups on the reorganization energy, The European Physical Journal D 73 (6) (2019) 1–8.
- [9] I. Arbouch, Y. Karzazi, B. Hammouti, Organic photovoltaic cells: operating principles, recent developments and current challenges—review, Physical and Chemical News 72 (2014) 73–84.
- [10] C. W. Tang, Two-layer organic photovoltaic cell, Applied physics letters 48 (2) (1986) 183–185.
- [11] J. Nelson, Organic photovoltaic films, Current Opinion in Solid State and Materials Science 6 (1) (2002) 87–95.
- [12] M. C. Scharber, N. S. Sariciftci, Efficiency of bulk-heterojunction organic solar cells, Progress in polymer science 38 (12) (2013) 1929–1940.
- [13] L. Aubouy, P. Gerbier, C. Guérin, N. Huby, L. Hirsch, L. Vignau, Study of the influence of the molecular organization on single-layer oleds' performances, Synthetic metals 157 (2-3) (2007) 91–97.
- [14] N. D. Colley, Computational and experimental investigations towards improving organic and dye-sensitized semiconductor solar cells, Ph.D. thesis, Southern Illinois University Carbondale (2016).
- [15] M. Jørgensen, K. Norman, F. C. Krebs, Stability/degradation of polymer solar cells, Solar Energy Materials and

Solar Cells 92 (2008) 686–714.

- [16] T. Sahdane, B. Kabouchi, A. Laghrabli, B. Azize, Photovoltaic energy conversion and optical properties of organic molecules based on aceanthraquinoxaline, *Der Pharma Chemica* 9 (1) (2017) 37–42.
- [17] Q. Meng, W. Hu, Recent progress of n-type organic semiconducting small molecules for organic field-effect transistors, *Physical Chemistry Chemical Physics* 14 (41) (2012) 14152–14164.
- [18] Z. Bao, A. J. Lovinger, J. Brown, New air-stable n-channel organic thin film transistors, *Journal of the American Chemical Society* 120 (1) (1998) 207–208.
- [19] Y. Sakamoto, T. Suzuki, M. Kobayashi, Y. Gao, Y. Fukai, Y. Inoue, F. Sato, S. Tokito, Perfluoropen-tacene: High-performance p-n junctions and complementary circuits with pentacene, *Journal of the American Chemical Society* 126 (26) (2004) 8138–8140.
- [20] H.-Y. Chen, I. Chao, Toward the rational design of functionalized pentacenes: reduction of the impact of functionalization on the reorganization energy, *ChemPhysChem* 7 (9) (2006) 2003–2007.
- [21] Y. Hu, J. Yin, K. Chaitanya, X.-H. Ju, Theoretical investigation on charge transfer properties of 1, 3, 5-tripyrrolebenzene (tpb) and its derivatives with electron-withdrawing substituents, *Croatica Chemica Acta* 89 (1) (2016) 81–90.
- [22] X. Wang, W. Pei, Y. Li, Enhancing charge transfer and photoelectric characteristics for organic solar cells, *Journal of Nanomaterials* 2020 (2020).
- [23] H. Li, X. Wang, Z. Li, Theoretical study of the effects of different substituents of tetrathiafulvalene derivatives on charge transport, *Chinese Science Bulletin* 57 (31) (2012) 4049–4056.
- [24] G. Nan, L. Wang, X. Yang, Z. Shuai, Y. Zhao, Charge transfer rates in organic semiconductors beyond first-order perturbation: From weak to strong coupling regimes, *The Journal of chemical physics* 130 (2) (2009) 024704.
- [25] D. L. Cheung, A. Troisi, Theoretical study of the organic photovoltaic electron acceptor pcbm: Morphology, electronic structure, and charge localization, *The Journal of Physical Chemistry C* 114 (48) (2010) 20479–20488.
- [26] N. G. Martinelli, J. Idé, R. S. Sánchez-Carrera, V. Coropceanu, J.-L. Brédas, L. Ducasse, F. Castet, J. Cornil, D. Beljonne, Influence of structural dynamics on polarization energies in anthracene single crystals, *The Journal of Physical Chemistry C* 114 (48) (2010) 20678–20685.
- [27] G. R. Hutchison, M. A. Ratner, T. J. Marks, Hopping transport in conductive heterocyclic oligomers: reorganization energies and substituent effects, *Journal of the American Chemical Society* 127 (7) (2005) 2339–2350.
- [28] M.-Y. Kuo, H.-Y. Chen, I. Chao, Cyanation: Providing a three-in-one advantage for the design of n-type organic field-effect transistors, *Chemistry—A European Journal* 13 (17) (2007) 4750–4758.
- [29] R. A. Marcus, Electron transfer reactions in chemistry. theory and experiment, *Reviews of Modern Physics* 65 (3)

(1993) 599.

- [30] V. Coropceanu, J. Cornil, D. A. da Silva Filho, Y. Olivier, R. Silbey, J.-L. Brédas, Charge transport in organic semiconductors, *Chemical reviews* 107 (4) (2007) 926–952.
- [31] J.-L. Brédas, J. P. Calbert, D. da Silva Filho, J. Cornil, Organic semiconductors: A theoretical characterization of the basic parameters governing charge transport, *Proceedings of the National Academy of Sciences* 99 (9) (2002) 5804–5809.
- [32] M. Mas-Torrent, P. Hadley, S. T. Bromley, X. Ribas, J. Tarrés, M. Mas, E. Molins, J. Veciana, C. Rovira, Correlation between crystal structure and mobility in organic field-effect transistors based on single crystals of tetrathiafulvalene derivatives, *Journal of the American Chemical Society* 126 (27) (2004) 8546–8553.
- [33] N. E. Gruhn, D. A. da Silva Filho, T. G. Bill, M. Malagoli, V. Coropceanu, A. Kahn, J.-L. Brédas, The vibrational reorganization energy in pentacene: molecular influences on charge transport, *Journal of the American Chemical Society* 124 (27) (2002) 7918–7919.
- [34] Z. Chen, Z. He, Y. Xu, W. Yu, Density functional theory calculations of charge transport properties of ‘plate-like’ coronene topological structures, *Journal of Chemical Sciences* 129 (9) (2017) 1341–1347.
- [35] Q. Liu, N. Gao, D. Liu, J. Liu, Y. Li, Structure and photoelectrical properties of natural photoactive dyes for solar cells, *Applied Sciences* 8 (9) (2018) 1697.
- [36] C. Sun, Y. Li, D. Qi, H. Li, P. Song, Optical and electrical properties of purpurin and alizarin complexone as sensitizers for dye-sensitized solar cells, *Journal of Materials Science: Materials in Electronics* 27 (8) (2016) 8027–8039.
- [37] C. Sun, Y. Li, P. Song, F. Ma, An experimental and theoretical investigation of the electronic structures and photoelectrical properties of ethyl red and carminic acid for dssc application, *Materials* 9 (10) (2016) 813.
- [38] J. Sun, Y. Wu, S. Dong, X. Li, W. Gao, Influence of the drying method on the bioactive compounds and pharmacological activities of rhubarb, *Journal of the Science of Food and Agriculture* 98 (9) (2018) 3551–3562.
- [39] N. Pan, G. Sun, *Functional textiles for improved performance, protection and health*, Elsevier, 2011.
- [40] P. Hohenberg, W. Kohn, Inhomogeneous electron gas, *Physical review* 136 (3B) (1964) B864.
- [41] A. D. Becke, Density-functional exchange-energy approximation with correct asymptotic behavior, *Physical review A* 38 (6) (1988) 3098.
- [42] C. Lee, W. Yang, R. G. Parr, Development of the colle-salvetti correlation-energy formula into a functional of the electron density, *Physical review B* 37 (2) (1988) 785.

- [43] A. D. Becke, Density-functional thermochemistry. i. the effect of the exchange-only gradient correction, *The Journal of chemical physics* 96 (3) (1992) 2155–2160.
- [44] D. Cagardová, V. Lukeš, Molecular orbital analysis of selected organic p-type and n-type conducting small molecules, *Acta Chimica Slovaca* 10 (1) (2017) 6–16.
- [45] H.-Y. Chen, I. Chao, Effect of perfluorination on the charge-transport properties of organic semiconductors: density functional theory study of perfluorinated pentacene and sexithiophene, *Chemical physics letters* 401 (4-6) (2005) 539–545.
- [46] K. Sakanoue, M. Motoda, M. Sugimoto, S. Sakaki, A molecular orbital study on the hole transport property of organic amine compounds, *The Journal of Physical Chemistry A* 103 (28) (1999) 5551–5556.
- [47] F. Sun, R. Jin, Dft and td-dft study on the optical and electronic properties of derivatives of 1,4-bis (2-substituted-1,3,4-oxadiazole) benzene, *Arabian Journal of Chemistry* 10 (2017) S2988–S2993.
- [48] S. Sahoo, S. Parida, S. Sahu, A theoretical study of charge transport properties of trifluoromethyl (-cf<sub>3</sub>) substituted naphthalene (tfmna) molecule, in: *IOP Conference Series. Materials Science and Engineering (Online)*, Vol. 149, 2016.
- [49] A. J. Prabha, T. Umadevi, P. Saranyac, G. Maheswari, R. Meenakshi, A complete theoretical study of indirubin-a blue dye for dye sensitized solar cells (dsscs) applications (2017).
- [50] R. E. Stratmann, G. E. Scuseria, M. J. Frisch, An efficient implementation of time-dependent density-functional theory for the calculation of excitation energies of large molecules, *The Journal of chemical physics* 109 (19) (1998) 8218–8224.
- [51] M. J. Frisch, G. W. Trucks, H. B. Schlegel, G. E. Scuseria, M. A. Robb, J. R. Cheeseman, G. Scalmani, V. Barone, B. Mennucci, G. A. Petersson, H. Nakatsuji, M. Caricato, X. Li, H. P. Hratchian, A. F. Izmaylov, J. Bloino, G. Zheng, J. L. Sonnenberg, M. Hada, M. Ehara, K. Toyota, R. Fukuda, J. Hasegawa, M. Ishida, T. Nakajima, Y. Honda, O. Kitao, H. Nakai, T. Vreven, J. A. Montgomery, Jr., J. E. Peralta, F. Ogliaro, M. Bearpark, J. J. Heyd, E. Brothers, K. N. Kudin, V. N. Staroverov, R. Kobayashi, J. Normand, K. Raghavachari, A. Rendell, J. C. Burant, S. S. Iyengar, J. Tomasi, M. Cossi, N. Rega, J. M. Millam, M. Klene, J. E. Knox, J. B. Cross, V. Bakken, C. Adamo, J. Jaramillo, R. Gomperts, R. E. Stratmann, O. Yazyev, A. J. Austin, R. Cammi, C. Pomelli, J. W. Ochterski, R. L. Martin, K. Morokuma, V. G. Zakrzewski, G. A. Voth, P. Salvador, J. J. Dannenberg, S. Dapprich, A. D. Daniels, Farkas, J. B. Foresman, J. V. Ortiz, J. Cioslowski, D. J. Fox, *Gaussian 09 Revision D.01*, Gaussian Inc. Wallingford CT 2009.
- [52] M. A. Spackman, D. Jayatilaka, Hirshfeld surface analysis, *CrystEngComm* 11 (1) (2009) 19–32.

- [53] D. Jayatilaka, D. J. Grimwood, Tonto: a fortran based object-oriented system for quantum chemistry and crystallography, in: International Conference on Computational Science, Springer, 2003, pp. 142– 151.
- [54] P. R. Spackman, M. J. Turner, J. J. McKinnon, S. K. Wolff, D. J. Grimwood, D. Jayatilaka, M. A. Spackman, Crystalexplorer: A program for hirshfeld surface analysis, visualization and quantitative analysis of molecular crystals, *Journal of Applied Crystallography* 54 (3) (2021).
- [55] J. Sancho-García, A. Pérez-Jiménez, Y. Olivier, J. Cornil, Molecular packing and charge transport parameters in crystalline organic semiconductors from first-principles calculations, *Physical Chemistry Chemical Physics* 12 (32) (2010) 9381–9388.
- [56] D. De Leeuw, M. Simenon, A. Brown, R. Einerhand, Stability of n-type doped conducting polymers and consequences for polymeric microelectronic devices, *Synthetic Metals* 87 (1) (1997) 53–59.
- [57] Saud I. Al-Resayes, Mohammad Azam, Agata Trzesowska-Kruszynska, Rafal Kruszynski, Saied M. Soliman, Ranjan K. Mohapatra, and Zahid Khan, Structural and Theoretical Investigations, Hirshfeld Surface Analyses, and Cytotoxicity of a Naphthalene-Based Chiral Compound, *ACS Omega* 5 (42) (2020) 27227-27234.
- [58] Pham Van Thong, Nguyen Thi Thanh Chi, Mohammad Azam, Cu Hong Hanh, Le Thi Hong Hai, Le Thi Duyen, Mahboob Alam, Saud I. Al-Resayes, Nguyen Van Hai, NMR investigations on a series of diplatinum(II) complexes possessing phenylpropenoids in CDCl<sub>3</sub> and CD<sub>3</sub>CN: Crystal structure of a mononuclear platinum complex, *Polyhedron*, 212 (2022), 115612,

# A DFT and TD-DFT Study on Emodin and Purpurin and their Functionalized Molecules to Produce Promising Organic Semiconductor Materials

---

ORIGINALITY REPORT

---

# 19%

SIMILARITY INDEX

---

PRIMARY SOURCES

---

1	<a href="https://link.springer.com">link.springer.com</a> Internet	102 words — 2%
2	Evgeniy V. Gromov, Irene Burghardt, Horst Köppel, Lorenz S. Cederbaum. " Impact of Sulfur vs Oxygen on the Low-Lying Excited States of -Coumaric Acid and - Coumaric Thio Acid ", The Journal of Physical Chemistry A, 2005 Crossref	76 words — 1%
3	<a href="https://arxiv.org">arxiv.org</a> Internet	71 words — 1%
4	<a href="https://cjoscience.com">cjoscience.com</a> Internet	52 words — 1%
5	<a href="https://www.mdpi.com">www.mdpi.com</a> Internet	39 words — 1%
6	<a href="https://cyberleninka.org">cyberleninka.org</a> Internet	33 words — 1%
7	<a href="https://pubs.rsc.org">pubs.rsc.org</a> Internet	31 words — < 1%
8	<a href="https://www.science.gov">www.science.gov</a> Internet	25 words — < 1%



- 
- 9 N. L. Janaki, B. Priyanka, Anup Thomas, K. Bhanuprakash. "A Computational Study of Semiconducting Benzobisthiazoles: Analysis of the Substituent Effects on the Electronic Structure, Solid-State Interactions, and Charge Transport Properties Using DFT Methods", *The Journal of Physical Chemistry C*, 2012  
Crossref 24 words — < 1%
- 
- 10 Focsan, Alexandrina Ligia. "EPR and DFT studies of proton loss from carotenoid radical cations", *Proquest*, 20111004  
ProQuest 22 words — < 1%
- 
- 11 [file.scirp.org](http://file.scirp.org)  
Internet 22 words — < 1%
- 
- 12 P. Akhileshwari, K. Sharanya, M. A. Sridhar. "Crystal Structure Characterization, Hirshfeld Surface Analysis, and Non-covalent Interactions of 2,5-Bis(4-chlorophenyl)-1,3,4-Oxadiazole", *Journal of Chemical Crystallography*, 2022  
Crossref 20 words — < 1%
- 
- 13 [academic-accelerator.com](http://academic-accelerator.com)  
Internet 20 words — < 1%
- 
- 14 Jie Feng, Hongshuai Wang, Nopporn Rujisamphan, Youyong Li. "Theoretical Design of Dithienopicenocarbazole-Based Molecules by Molecular Engineering of Terminal Units Toward Promising Non-fullerene Acceptors", *Frontiers in Chemistry*, 2020  
Crossref 19 words — < 1%
- 
- 15 Chen, H.Y.. "Effect of perfluorination on the charge-transport properties of organic semiconductors: density functional theory study of 18 words — < 1%

perfluorinated pentacene and sexithiophene", Chemical Physics Letters, 20050111

Crossref

16 Suh, Yong Jae, Jin Wook Chae, Hee Dong Jang, and Kuk Cho. "Role of chemical hardness in the adsorption of hexavalent chromium species onto metal oxide nanoparticles", Chemical Engineering Journal, 2015. 17 words — < 1%

Crossref

17 silo.pub 17 words — < 1%

Internet

18 Rowa Oshi, Sahar Abdalla, Michael Springborg. "Theoretical study on functionalized anthracene and tetraceneas starting species to produce promising semiconductor materials", Computational and Theoretical Chemistry, 2018 16 words — < 1%

Crossref

19 Shashank Masaldan, Vidhya V. Iyer. "Exploration of effects of emodin in selected cancer cell lines: enhanced growth inhibition by ascorbic acid and regulation of LRP1 and AR under hypoxia-like conditions", Journal of Applied Toxicology, 2014 16 words — < 1%

Crossref

20 Yin, Jun, Kadali Chaitanya, and Xue-Hai Ju. "Theoretical investigation of fluorination effect on the charge carrier transport properties of fused anthra-tetrathiophene and its derivatives", Journal of Molecular Graphics and Modelling, 2016. 16 words — < 1%

Crossref

21 onlinelibrary.wiley.com 16 words — < 1%

Internet

---

22 Denisa Cagardová, Vladimír Lukeš. "Molecular orbital analysis of selected organic p-type and n-type conducting small molecules", Acta Chimica Slovaca, 2017 15 words — < 1%  
Crossref

---

23 Yuanchao Li, Yuguang Lv, Yunpeng Liu, Hongbing Gao, Qi Shi, Yuanzuo Li. "DFT and TD-DFT investigations of organic dye with different  $\pi$ -spacer used for solar cell", Journal of Materials Science: Materials in Electronics, 2017 15 words — < 1%  
Crossref

---

24 Mahdavifar, Zabiollah, and Hoda Salmanizadeh. "A quantum chemical study of the factors influencing performance of DTTTD: Fullerene heterojunction photovoltaic models", Journal of Photochemistry and Photobiology A Chemistry, 2015. 13 words — < 1%  
Crossref

---

25 Pooja S. Singh, Purav M. Badani, Rajesh M. Kamble. "Blue-orange emitting carbazole based donor-acceptor derivatives: Synthesis and studies of modulating acceptor unit on opto-electrochemical and theoretical properties", Journal of Photochemistry and Photobiology A: Chemistry, 2021 13 words — < 1%  
Crossref

---

26 Song, Peng, Yuanzuo Li, Fengcai Ma, Tõnu Pullerits, and Mengtao Sun. "External Electric Field-Dependent Photoinduced Charge Transfer in a Donor-Acceptor System for an Organic Solar Cell", The Journal of Physical Chemistry C, 2013. 12 words — < 1%  
Crossref

---

27 scholarworks.bwise.kr 12 words — < 1%  
Internet

- 
- 28 vital.seals.ac.za:8080 12 words — < 1%  
Internet
- 
- 29 www.coursehero.com 12 words — < 1%  
Internet
- 
- 30 Chia-Chun Liu, Shih-Wei Mao, Ming-Yu Kuo. "Cyanated Pentaceno[2,3- ]chalcogenophenes for Potential Application in Air-Stable Ambipolar Organic Thin-Film Transistors ", The Journal of Physical Chemistry C, 2010 11 words — < 1%  
Crossref
- 
- 31 Hsing-Yin Chen. "Toward the Rational Design of Functionalized Pentacenes: Reduction of the Impact of Functionalization on the Reorganization Energy", ChemPhysChem, 09/11/2006 11 words — < 1%  
Crossref
- 
- 32 Li, Ping, Yahui Cui, Chongping Song, and Houyu Zhang. "Effects of Sulfur Oxidation on the Electronic and Charge Transport Properties of Fused Oligothiophene Derivatives", The Journal of Physical Chemistry C 11 words — < 1%  
Crossref
- 
- 33 Ling Liu, Guochun Yang, Yun Geng, Yong Wu, Zhongmin Su. "Electron transport via phenyl-perfluorophenyl interaction in crystals of fluorine-substituted dibenzalacetones", RSC Adv., 2014 11 words — < 1%  
Crossref
- 
- 34 Masoudi, Mohaddeseh, Mahdi Behzad, Ali Arab, Atekeh Tarahhomi, Hadi Amiri Rudbari, and Giuseppe Bruno. "Crystal structures, DFT calculations and Hirshfeld surface analyses of three new cobalt(III) Schiff base complexes derived from meso-1,2-diphenyl-1,2-ethylenediamine", Journal of Molecular Structure, 2016. 11 words — < 1%

35 Nuha Wazzan, Ahmad Irfan. "Exploring the optoelectronic and charge transport properties of Pechmann dyes as efficient OLED materials", *Optik*, 2019

Crossref

11 words — &lt; 1%

36 R. Nithya, M. Sowmiya, P. Kolandaivel, K. Senthilkumar. "Structural, optical, and charge transport properties of cyclopentadithiophene derivatives: a theoretical study", *Structural Chemistry*, 2013

Crossref

11 words — &lt; 1%

37 S. Gunavathi, R. Venkateswaramoorthi, K. Arulvani, S. Bharanidharan. "Synthesis and characterisation of formohydrazide derivatives as potential antimicrobial agents: molecular docking and DFT studies", *Molecular Physics*, 2022

Crossref

11 words — &lt; 1%

38 Souad DEKAR, Moufida MERZOUGUI, Jean WEISS, Kamel OUARI. "Structural investigations and catalytic performances of a new oxovanadium complex derived from 1, 2-bis ((E)-5-bromo-2-hydroxybenzylidèneamino)-4-methyl benzene.", *Journal of Molecular Structure*, 2022

Crossref

11 words — &lt; 1%

39 [essayhelpp.com](http://essayhelpp.com)

Internet

11 words — &lt; 1%

40 Gohel, Khushbu N.. "Electrochemical Properties of Nanocomposite Polymer Blend Gel Electrolytes for Battery Applications", Maharaja Sayajirao University of Baroda (India), 2021

ProQuest

10 words — &lt; 1%

41 Hao - Jung Chang, Mykhailo V. Bondar, Natalia Munera, Sylvain David et al. "Femtosecond

10 words — &lt; 1%

## Spectroscopy and Nonlinear Optical Properties of aza - BODIPY Derivatives in Solution", Chemistry – A European Journal, 2022

Crossref

42 Rowa Oshi, Sahar Abdalla, Michael Springborg. "Study of the influence of functionalization on the reorganization energy of naphthalene using DFT", Computational and Theoretical Chemistry, 2017 10 words — < 1%

Crossref

43 Sancho-García, Juan Carlos, Mónica Moral, and Ángel José Pérez-Jiménez. "The Effect of Cyclic Topology on Charge-Transfer Properties of Organic Molecular Semiconductors: The Case of Cycloparaphenylene Molecules", The Journal of Physical Chemistry C 10 words — < 1%

Crossref

44 Springer Series in Materials Science, 2015. 10 words — < 1%

Crossref

45 Xiaorui Liu, Chengzhi Huang, Wei Shen, Rongxing He, Ming Li. "Theoretical Investigation of Donor-Acceptor Copolymers Based on C-, Si-, and Ge-Bridged Thieno[3,2-b]dithiophene for Organic Solar Cell Applications", Journal of Electronic Materials, 2016 10 words — < 1%

Crossref

46 Ayhan Üngördü. "Charge transfer properties of Gaq3 and its derivatives: An OLED study", Chemical Physics Letters, 2019 9 words — < 1%

Crossref

47 Bavita Kumari, Kiran Singh, Amit Sharma. "Synthesis, crystal structure and molecular docking studies of novel Schiff base ligand 9-(((3-ethyl-5-mercapto/thio-4H-1,2,4-triazole-4-yl)imino)methyl)-anthracene and its complexes with Ni(II), Cu(II), Zn(II) and Cd(II): Comparative 9 words — < 1%

spectral, thermo-kinetics, radical scavenging and antimicrobial studies", Chemical Data Collections, 2022

Crossref

48 Huong, Vu Thi Thu, Truong Ba Tai, and Minh Tho Nguyen. "Theoretical Design of n-Type Organic Semiconducting Materials Containing Thiazole and Oxazole Frameworks", The Journal of Physical Chemistry A, 2014. 9 words — < 1%

Crossref

49 Jun-Rong CHEN. "DFT Study on the Effect of Different Peripheral Chains on Charge Transport Properties of Triphenylene Derivatives", Chinese Journal of Chemistry, 12/2008 9 words — < 1%

Crossref

50 Urgut, O.S., I.I. Ozturk, C.N. Banti, N. Kourkoumelis, M. Manoli, A.J. Tasiopoulos, and S.K. Hadjikakou. "New antimony(III) halide complexes with dithiocarbamate ligands derived from thiuram degradation: The effect of the molecule's close contacts on in vitro cytotoxic activity", Materials Science and Engineering C, 2016. 9 words — < 1%

Crossref

51 Ya-Rui, Shi, Wei hui-ling, and Liu Yu-Fang. "Research on charge-transport properties of TTF-TTP derivatives and organic interfaces", RSC Advances, 2016. 9 words — < 1%

Crossref

52 Yuanzuo Li, Beibei Xu, Peng Song, Fengcai Ma, Mengtao Sun. "D-A- $\pi$ -A System: Light Harvesting, Charge Transfer, and Molecular Designing", The Journal of Physical Chemistry C, 2017 9 words — < 1%

Crossref

53 aip.scitation.org 9 words — < 1%

Internet

- 
- 54 [lab409.chem.ccu.edu.tw](http://lab409.chem.ccu.edu.tw) Internet 9 words — < 1%
- 
- 55 [tel.archives-ouvertes.fr](http://tel.archives-ouvertes.fr) Internet 9 words — < 1%
- 
- 56 [www.intechopen.com](http://www.intechopen.com) Internet 9 words — < 1%
- 
- 57 [www.sid.ir](http://www.sid.ir) Internet 9 words — < 1%
- 
- 58 "Electron Transfer in Chemistry", Wiley, 2001 Crossref 8 words — < 1%
- 
- 59 A. Venkateswararao, K. R. Justin Thomas, Chuan-Pei Lee, Chun-Ting Li, Kuo-Chuan Ho. "Organic Dyes Containing Carbazole as Donor and  $\pi$ -Linker: Optical, Electrochemical, and Photovoltaic Properties", ACS Applied Materials & Interfaces, 2014 Crossref 8 words — < 1%
- 
- 60 Harjinder Singh. "Crystal structure, surface analysis, and computational investigations of 1-(4-chloro-3-nitrophenyl)-6,7-dihydro-1H-benzo[d][1,2,3]triazol-4(5H)-one as potential acceptor molecule for photovoltaics applications", Journal of Molecular Structure, 2022 Crossref 8 words — < 1%
- 
- 61 Jin, R.. "Theoretical study of chemosensor for fluoride and phosphate anions and optical properties of the derivatives of 2-(2-hydroxyphenyl)-1,3,4-oxadiazole", Chemical Physics, 20110228 Crossref 8 words — < 1%
- 
- 62 Ming-Yu Kuo. "Cyanation: Providing a Three-in-One Advantage for the Design of n-Type Organic Field- 8 words — < 1%



63 Shamsa Bibi, Ping Li, Jingping Zhang. "X-Shaped donor molecules based on benzo[2,1-b:3,4-b']dithiophene as organic solar cell materials with PDIs as acceptors", Journal of Materials Chemistry A, 2013  
8 words — < 1%  
Crossref

64 [chemistry-europe.onlinelibrary.wiley.com](http://chemistry-europe.onlinelibrary.wiley.com)  
Internet  
8 words — < 1%

65 [dspace.ncl.res.in:8080](http://dspace.ncl.res.in:8080)  
Internet  
8 words — < 1%

66 [etd.gatech.edu](http://etd.gatech.edu)  
Internet  
8 words — < 1%

67 [nbo7.chem.wisc.edu](http://nbo7.chem.wisc.edu)  
Internet  
8 words — < 1%

68 [nozdr.ru](http://nozdr.ru)  
Internet  
8 words — < 1%

69 [repositorio.upct.es](http://repositorio.upct.es)  
Internet  
8 words — < 1%

70 [uomphysics.net](http://uomphysics.net)  
Internet  
8 words — < 1%

71 [worldwidescience.org](http://worldwidescience.org)  
Internet  
8 words — < 1%

72 [www.asianjournalofchemistry.co.in](http://www.asianjournalofchemistry.co.in)  
Internet  
8 words — < 1%

73 Asif Mahmood, Ahmad Irfan. "Effect of fluorination on exciton binding energy and electronic coupling in small molecule acceptors for organic solar cells", Computational and Theoretical Chemistry, 2020

Crossref

7 words — < 1%

74 Ramalingam, M.. "C-H functionalisation through carbene and fluorocarbene insertion-ab initio and DFT investigations", Journal of Molecular Structure: THEOCHEM, 20051130

Crossref

7 words — < 1%

75 Shafiq UrRehman, Makhvela Anwer, Shamsa BiBi, Saba Jamil, Muhammad Yasin, Shanza Rauf Khan, RaziyaNadeem, Sarmed Ali, Ran Jia. "DFT analysis of different substitutions on optoelectronic properties of carbazole-based small acceptor materials for Organic Photovoltaics", Materials Science in Semiconductor Processing, 2022

Crossref

7 words — < 1%

76 Xian-Kai Chen, Jing-Fu Guo, Lu-Yi Zou, Ai-Min Ren, Jian-Xun Fan. " A Promising Approach to Obtain Excellent -Type Organic Field-Effect Transistors: Introducing Pyrazine Ring ", The Journal of Physical Chemistry C, 2011

Crossref

7 words — < 1%

77 "Organic Semiconductors for Field-Effect Transistors", Lecture Notes in Chemistry, 2015.

Crossref

6 words — < 1%

78 Asha Sharma, U. Lourderaj, Deepak, N. Sathyamurthy. "Determination of Stability and Degradation in Polysilanes by an Electronic Mechanism", The Journal of Physical Chemistry B, 2005

Crossref

6 words — < 1%

---

79 J. Christina Jebapriya, Johanan Christian Prasana, S. Muthu, B. Fathima Rizwana. "Spectroscopic (FT-IR and FT-Raman), quantum computational (DFT) and molecular docking studies on 2(E)-(4-N,N-dimethylaminobenzylidene)-5-methylcyclohexanone", Materials Today: Proceedings, 2020

Crossref

---

80 Jun Yin, Kadali Chaitanya, Xue-Hai Ju. "Bromination and cyanation for improving electron transport performance of anthra-tetrathiophene", Journal of Materials Research, 2016

Crossref

---

81 Rowa Oshi, Sahar Abdalla, Michael Springborg. "The impact of functionalization of organic semiconductors by electron donating groups on the reorganization energy", The European Physical Journal D, 2019

Crossref

---

82 Smith, Andrew Gregory. "Investigation of Organic Dyes for Dye-Sensitized and Organic Solar Cell Applications.", Baylor University, 2018

ProQuest

---

83 Yahong Zhang, Yuping Duan, Jia Liu, Daoyuan Zheng, Mingxing Zhang, Guangjiu Zhao. "Influence of the Halogenated Substituent on Charge Transfer Mobility of Aniline Tetramer and Derivatives: Remarkable Anisotropic Mobilities", The Journal of Physical Chemistry C, 2017

Crossref

---

EXCLUDE QUOTES OFF

EXCLUDE MATCHES OFF

EXCLUDE BIBLIOGRAPHY ON